Novel Non-Intrusive Trans-Dermal Remote Wireless Micro-Fluidic Monitoring System Applied to Continuous Glucose and Lactate Assays for Casualty Care and Combat Readiness Assessment

John F. Currie*, Michael M. Bodo, Frederick J. Pearce
Department of Resuscitative Medicine, Walter Reed Army Institute of Research,
503 Robert Grant Avenue, Silver Spring, MD. 20910-7500, USA
*and Physics Department, GAEL, Georgetown University, Washington DC 20057-0995, USA

john.currie@na.amedd.army.mil, michael.bodo@na.amedd.army.mil, frederick.pearce@na.amedd.army.mil

ABSTRACT

We present results on both the bio-medical engineering development of a non-intrusive, wireless, micro-fluidic physiological monitoring and remote transmission field system, and its performance measuring continuous glucose and lactate concentrations in the interstitial fluid of rats subjected both to glucose-stress tests, and to hemorrhagic shock. These directly address the two symposium topics of "Monitoring of physiological parameters and measurement of vital signs in the field" and of "Medical surveillance in a command environment, remote monitoring and guidance of field personnel".

1.0 INTRODUCTION

1.1 Relevance to the Symposium

Glucose and lactate concentration variations have been documented in the compensatory and de-compensatory phases of shock. A detailed, continuous, and precise knowledge of these concentrations in an individual can provide many advantages to combat casualty care personnel and emergency medical surgeons. These include individual healthy baselines, information for triage, and monitoring the physiological evolution of shock so as to pinpoint optimal stabilization and resuscitative treatment strategies. The prototype system we have created provides this advanced diagnostic aid and decision support using the most recent technology for remote wireless electronics and novel non-intrusive sampling based on micro-fluidics.

1.2 Description of Methods Employed and Results Obtained

With DARPA support[1], we have fabricated a prototype micro-fluidic platform system[2], called BFIT (**B**io-**F**luidic **I**ntegrated **T**ransdermal Microsystem), for the ***non-intrusive***, sequential, real-time trans-dermal sampling & analysis of molecules that ordinarily do not diffuse across the skin, such as polar molecules. The BFIT provides an individual, personal baseline while being both disposable and sterile. Our approach employs the non-invasive sampling of living tissue, in a unique and minimally disruptive fashion, retrieving an

Paper presented at the RTO HFM Symposium on "Combat Casualty Care in Ground Based Tactical Situations: Trauma Technology and Emergency Medical Procedures", held in St. Pete Beach, USA, 16-18 August 2004, and published in RTO-MP-HFM-109.

insignificant volume of interstitial fluid (<<10 ng). The monitoring is time controlled and can cover short- or long-term time periods (days-months). It is an absolute measurement with no need for an external or on-board glucose reference. Finally, it can be generalized to monitoring almost any moderately hydrophilic/soluble bio-molecule of molecular weight less than 60k Daltons, as are commonly found in measurable concentrations in the interstitial fluid just under the skin's stratum corneum. Biologically, we sample, analyze and record the concentration of glucose and of lactate in the interstitial fluid as a stress and shock/trauma physiological indicator. We have proven both optical and electrical implementations of the transduction technology. Finally, we have adapted wireless control circuitry (RRAPDS), currently used in the field to monitor Army missiles and munitions, to the control and remote reporting of the BFIT's glucose and lactate assays. Here we present physiological data obtained from controlled animal experiments on healthy rats, and on rats in shock, comparing our data with periodic blood-gas assays obtained from whole shed blood.

1.2 Military Significance (Resuscitative Medicine / Casualty Care)

The potential to be successfully resuscitated from severe traumatic hemorrhagic shock is time-critical for both combat casualties and civilian trauma victims with traumatic exsanguinations. There are a number of critical care medicine research areas[3] in which nonintrusive quasi continuous field deployable monitors would greatly benefit successful resuscitation. First, for both triage and effective treatment, there is the pin-pointing exactly the moment in the shock time course the casualty is found by medics. Work by Pearce et al.[4] documents the typical hematocrit, plasma glucose and lactate values observed during the hemorrhagic shock and identifies four progressive phases: i) early compensatory (homeostatic mechanisms), ii) maximal compensatory, iii) early decompensatory (during blood re-infusion, close to irreversibility) and iv) late decompensatory (leading to death). If resuscitative fluids can be administered before the late compensatory phase when organs such as kidneys and the liver are ischemic, and there is severe acidosis, then survivability is high. There is evidence[3] that small volumes of glucose infusions (or iso- or hyper-tonic saline, or hespan, not blood) can both moderate systemic acidosis as well as delay the onset of the fatal decompensation phases. From a research point of view, a quasi-continuous monitor (e.g. a reading every 1 - 2 minutes) would also shed light on the efficacies of both the volume and composition of the resuscitation fluid employed. Thirdly, to know even more precisely where one individual is situated on the compensatory/decompensatory time course, one must have a "baseline" prior to injury of that individual's plasma glucose and lactate (even alcohol) concentrations which can be significantly altered from normal rest values by extreme stress and exertion as encountered in combat. In this context, nonintrusive monitoring of glucose and lactate, of each individual warfighter with an unobtrusive band-aid like device throughout combat, from rest to exertion and possible injury, is highly desirable. It is only the frequency of sampling which changes from infrequent, to frequent, to quasi-continuous in the case of casualty when the monitoring device then serves as both a triage and a critical care instrument. Combined with other physiological instruments under development in the Warfighter Physiological Status Monitoring suite,[5] a complete picture is available for a commander, a medic or a field surgeon.

2.0 THE BFIT MICROSYSTEM

2.1 System Components

The microsystem consists of four major components, each of which have been developed separately and are now being demonstrated in an integrated fashion. Referring to the lettered features of the photographs in Figure 1 below, we see A) Flexible disposable micro fluidic electro-chemical chip with multiple sensor cells, B) Flexible disposable micro fluidic optical chip, C) Flexible cable and connector, D) Wireless control and

messaging unit (modified US Army, 100 m range), E) Wireless Integrator computer, ***or*** node of Land Warrior's computer; F) ultimate integration goal for A, C & D on an equipment band or strap ('05). We discuss some of the unique engineering that went into the BFIT sampling chip below.

Figure 1. Photographs of the demonstration BFIT microsystem. See the text above for identification of the lettered features.

2.2 BFIT Sampling Chip

The BFIT sampling chip is a flexible patch-like chip with a multilayer polymeric metal laminate structure and was fabricated using SU-8 as a structural layer[6,7,8], a Teflon-AF release layer[9], polymethylmethacrylate (PMMA)[10], polypyrrole (PPy) and glucose oxidase (GOD). The BFIT fabrication process uses SU8 as a principal structural material consisting of five steps (Figure 2). This process is a subset of an earlier technology developed for the polymer material PDMS.[11,12,13,14,15] The first step was the deposition of a Teflon release layer on a glass substrate, which allowed the multi-layered multi polymeric devices to be removed easily from the glass after fabrication. A thin layer of SU8 was formed by spin coating and acted as a base layer (10 μ) for the rest of the device and provided adhesion to the Teflon. The third step in the fabrication process consisted of spin coating a thick (150 μ) SU8 layer. This thick layer provided the structural support for the device. Chromium/gold electrode/heater metallization (0.5 μ) was sputtered deposited and patterned on top of the thick SU8 (150 μ) layer. 10μ PMMA was then spun coated as a protective layer for the selective deposition of PPy and enzyme. In order to prevent electrode pads getting covered by PMMA, scotch tape was applied on the electrode pads prior to PMMA spin was removed before PMMA baking process. PMMA layer was further selectively plasma etched in such a way that only one of the electrodes was exposed and the other electrode was covered (Figure 3). The metals were patterned using positive photo-resist and wet-chemical etching. Before the sputter deposition, a plasma surface treatment was employed to improve the adhesion between the SU8 and the metal layers. Releasing the device from the glass substrate using a razor blade was the next step. The release layer was formed by spin coating a solution of amorphous fluoropolymers (Teflon) diluted with perfluorinated solvent

Glucose oxidase (GOD), the current enzyme prototype, was adsorbed electrochemically onto a polypyrrole (PPy) layer using a potentiostat together with an electrolyte solution consisting of 0.1 M, each, of PPy and KCl at 0.8 V for 2 minutes. 0.1 M Ferricyanide and 8001 units/ml of GOD (18 μl GOD and 48 μl K3FeCN6 in 10 ml phosphate buffer solution) were further added in the electrolyte solution for the deposition of GOD. Selective deposition of Ppy + GOD was then done on one of the exposed electrodes of the B-IT cell (Figure 3). Chronoamperometric dose responses were recorded and the results revealed that the sensor had a good linearity from 0 to 10 mM glucose with the sensitivity of 2.9 mA/mM. For our lactate sensor chips we use the same process except we substitute lactate oxidase for the GOD.

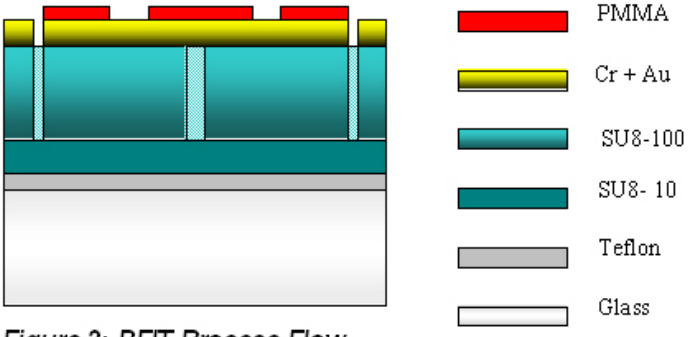

Figure 2: BFIT Process Flow

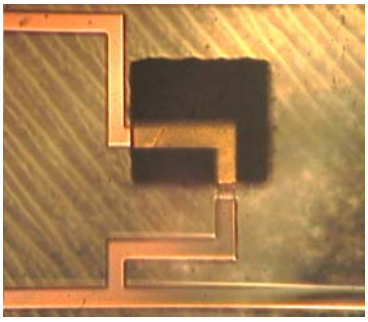

Figure 3: Top view photograph of a single B-IT cell showing selective deposition of PPy + GOD

2.2 Connector/Cabling

We modified the design of our glucose and lactate chips to make them compatible with a new generation of zero-insertion force (ZIF) connectors made by Kyocera. Chip thicknesses were adjusted to be 150µm +/- 10 µm for optimal insertion reproducibility and the connector pad pin-outs were drawn to meet with the 300-pitch staggered connector positions. Most important is the ability to make "bottom" chip contacts allowing a flat connector and chip surface that can be pressed to the body of the subject. That is, there is no step in level at the connector body that prevents a good flat contact with the skin. The body of the connector is 1.8 mm high in a surface mountable dual in-line package and is equipped with a ZIF slider mechanism that locks the chip into place once correctly inserted. We have seen that this allows us to change BFIT sensor chips reproducibly in a minute, yet be study enough to accept multiple insertions and to resist forces that would withdraw the chip from the socket due to the normal movement of the animal under experimental study. The part is made in different widths corresponding to a range of 17 to 91 pin contacts. We have used the ones for 31 and 61 pins in our development work. The connector photographed in Figures 1, 7D, 8G, and 8H is the 61 pin version soldered to a wire cable. We have also used in with flexible multi-conductor kapton tapes as shown in Figure 1C. In the integrated device shown in Figure 1F this connector is rigidly connected to the body of the control electronics package. The connector is available in both tape and reel-to-reel packages for economic automated assembly and manufacture.

2.3 Control Electronics

The control electronics used in this study have been made by Holeman Scientific Corporation[16] of Huntsville Alabama with support from the DARPA/ARO grant (Ref.1). It is a modification of electronics developed by the Redstone Arsenal's RDEC used to monitor the readiness and functioning of missiles and of munitions. The electronics consists of two parts. The first is a computer-interfaced wireless data collection system that is capable of addressing up to 64 remote sensor nodes managing the identification of each one as well as interrogating each one for the contents of its memory buffers. The second part is the sensor node. It is made up of five functional parts: RF communication (with unique identification), a microprocessor controller, a multiplexer, analog circuit sources and A/D converters, and multiple sensor input. The modifications made by Holeman concern principally programming the microprocessor, and adapting the analog circuits, multiplexer and input lines to our device. The details of this electrical engineering will be given elsewhere. Of importance is that the range of communication is about 300 m to allow communication between a command center and members of a platoon. Each soldier can be monitored individually for glucose and lactate concentrations. If the soldier is healthy, an individual rested baseline can be measured and stored. As the soldier exerts himself the blood glucose and lactate levels can be monitored. Extreme exerting can be seen in hypoglycemia and

elevated lactate levels. This physiological state affects the soldier's ability to perform in battle or subsequent situations of high exertion. If the soldier suffers a casualty, the monitors can be activated to measure quasi-continuously as shown in the studies below, and the micro system behaves as a critical care and triage instrument.

2.4 Overview of System Specifications for BFIT and CGMS Systems used in this Study

Sensor		
Component	BFIT Performance Specifications	MINIMED CGMS Performance Specifications
Glucose Sensor	NONINTRUSIVE: OK for > 7 days. There is no inflammation. Micro-pores heal in hours.	Designed to be worn by the patient up to 3 days;
	storage lifetime dry > 4 months	refrigerated, 1 mo max lifetime
	Accuracy: <20%	Accuracy <20%
	Drift: <0.2%/h	Drift: sometimes a problem; replace
	Calibration: by batch	Calibration: multiple finger sticks
Lactate Sensor	in development	none
Monitor		
Component	BFIT Performance Specifications	MINIMED CGMS Performance Specifications
Glucose Measurement Range	20- 1000 mg/dl;	40-400 mg/dl
Typical Operating Range	>1200 ft. (300 m)	6 ft. (2 m)
Display Window Length:	PC-based currently: to screen resolution	1.40 in : 0.70 in
Dimensions Length:	breadboard prototype 3 in : 3 in : 1 in	3.56 in : 2.77 in : 0.08 in
Weight	Prototype: 2.8 oz; miniaturizing to 0.5 oz.	4 oz (114 grams)
Warranty	prototype; Electronics MILSPEC reliable >10 yrs in US Army Missile Command	1 year
System Memory	Monitor stores 1k readings to RF-download	Stores up to 21 days of data
Alarms Audible	PC-based currently, using PC speakers	(50 decibels @ 1 meter) Optional Vibrate Mode
Batteries	Prototype Transmitter Monitor uses (2) AAA alkaline batteries. Battery life >1 mo. Miniaturizing to 3 V Li cell	The Monitor uses (2) AAA alkaline batteries. Battery life exceeds 1 mo under normal use
Frequency	1 measurements: 30 seconds; variable intervals	1 measurement per 5 min (300 sec); fixed interval
Transmitter		
Component	BFIT Performance Specifications	MINIMED CGMS Performance Specifications
Body Compatibility	NONINTRUSIVE	Complies with ISO 10993-1 long-term contact
Transmitter Life	prototype; Electronics reliable >10 yrs	1 year under anticipated normal use conditions
Electrochemical Detection		
Component	BFIT Performance Specifications	MINIMED CGMS Performance Specifications
GOD Enzyme anchor	electrochemically deposited polypyrrole	optically exposed hydrogel
Response Time [s]	1	10; time averaged to 300
Electrode Area [mm^2]	0.07	0.3
Stability	Drift: <0.2%/h	sometimes 100%/h

Table 1. BFIT and CGMS comparative system specifications.

2.5 System Operation Overview

Each measuring chip currently has 25 individual measuring cells that are addressed individually and sequentially by the control electronics. The number 25 was chosen arbitrarily for demonstration purposes. These cells are designed into a 5x5 array. We could practically integrate 100 in a 10x10 array with little technical challenge, and perhaps ultimately as many as 1600 in a $1cm^2$ area. Each cell has a heater element

that is used to ablate the stratum corneum, and then is fused to create an open circuit. The microprocessor of the sensor node electronics selects one cell with the multiplexer and then applies a train of controlled electrical pulses of precise energy and voltage to perform the ablation and fuse the heater wire. One of the arms of the conductive gold metal paths leading to the heater has been selectively deposited with a polymer matrix containing either GOD or LOD enzymes. The other arm is left bare. Together they form a two-electrode electrochemical cell selectively sensitive to glucose of lactate. The sensor node electronics then applies a voltage pulse of 0.2 V for duration of up to 30 s and precisely measures the current flowing at a programmable time following the application. We have waited 10 s before measuring the current to ensure that the current transients have all attenuated. This current measurement can be repeated indefinitely until the cell no longer registers a current. As we will see below this cell lifetime varies from a few minutes to a few hours. We are working to increase this lifetime to a day or more. When one cell no longer responds the next one in the sequence can be opened. With some program modifications we have been able to open and follow up to three cells that are open at the same time to check in real time for reproducibility in the measured response. More on the technical engineering details will be published elsewhere.

3.0 IN-VITRO EXPERIMENTS, CALIBRATION

After fabrication, BFIT sensor chips are calibrated for sensitivity in composition controlled solutions. Figure 4 below shows the results of chronoamperometric calibrations over an hour of one typical cell of the 25 on a sensor chip as the ambient glucose concentration is increased in 10 mmol steps every 10 min from 0 to 50 mM. The calibrations are performed using a 50 cc vial containing the sensor chip under test bathing in isotonic phosphate-buffered 5% saline solution. In each case we add measured volumes of concentrated glucose and mix with a small stirring bar located in the bottom of the vial for 8 min. When agitation stops we perform an I-t sweep over a 30 s period, first grounding the electrodes, then applying a 30 s 0.2 V potential between them and record the electrochemical current. The observed current pulse reaches a peak value in milliseconds and relaxes exponentially to an equilibrium value of 0.1 – 1.0 mA for the electrode areas of 0.07 mm^2 we employ. At any instant the current is proportional to the glucose concentration. Practically, we wait 10 sec from the beginning of the voltage pulse before recording the current. In Figure 6, we plot this current as a function of the precise ambient glucose concentration as a calibration curve in the physiologically sensitive 1-10 mM range. Note that our devices have a linear calibration curve, saturating in concentrations far above 50 mM.

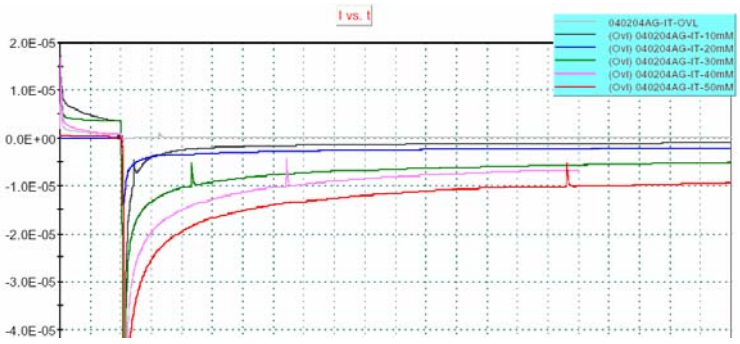

Figure 4 Chronoamperometric responses of a PPY-GOX-ferri film in in the absence and presence of Glucose Glucose

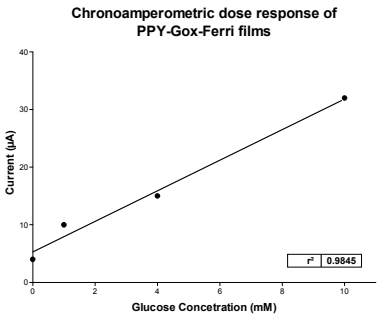

Figure 5 Dose response of PPY-GOX-ferri film response to varying amounts of

We employ a similar calibration procedure with our lactate chips. They too are linear in the physiologically important concentration range of 0.1 – 20 mM.

4.0 IN-VIVO EXPERIMENTS

4.1 Animal Experiment Overview

Research was conducted in compliance with the Animal Welfare Act and other federal statutes and regulations relating to animals and experiments involving animals and adheres to principles stated in the Guide for the Care and Use of Laboratory Animals, NRC Publication, 1996 edition.

Animal experiments were all performed under approved hemorrhagic shock protocols at the Walter Reed Army Institute of Research as amendments to ongoing research programs. Some of the details of the protocols as well as the results of those experiments appear in the subsequent papers in these proceedings[17]. The modifications permitted us to add i) our nonintrusive glucose and lactate monitoring microsystem developed for diabetics (MiniMed-CGMS), ii) a commercial intrusive, subcutaneous glucose monitor, iii) either IP injection or arterial artery infusion of glucose for glucose stress testing, iv) a laser-Doppler probe to measure circulation in the immediate vicinity of the BFIT placement throughout the hemorrhagic shock, and v) to measure 1 ml of the frequently drawn arterial blood samples in a precision glucose and lactate assay system (YSI-2700). The animals used were both Sprague-Dawley rats (both male and female, 250-350g) and male pigs (65-80 kg).

Both rats and pigs are good animal choices to demonstrate our monitoring micro-system, and in particular the BFIT sampling chip. The pig's skin and physiology are very close to those of the human, although the stratum corneum is rougher and thicker than human's. Despite the fur and the lack of sweating, the rat's skin too is a useful model to living human skin since the stratum corneum is smooth and the same thickness as humans. Rat fur must be carefully shaved-away on its abdomen using a micro-screen razor so that no cutting edge scrapes and inflames the skin or disrupts the stratum corneum. The same technique was used to trim and remove the sparse but wiry hairs on the pig's inner thighs where we placed the BFIT sensors.

At the time of writing, we have completed three pairs of experiments. In the first, we performed two hemorrhagic shock experiments with glucose stress-testing on rats. One involved an arterial glucose injection following resuscitation of a female rat (R16 – these numbers refer to animal numbers used in the protocols[18] of Baranyi and Lee), the other involved two glucose arterial injections prior to controlled hemorrhagic shock, and a third following resuscitation of a male rat (R226). The second pair of experiments was performed on two male rats who were administered 0.1 mg of theophylline intra-arterially 10 min prior to beginning the hemorrhagic shock. The third pair of experiments was performed on two male pigs who were subjected to two hemorrhagic shock cycles with resuscitation using isotonic saline.

In all experiments glucose concentrations were monitored with the BFIT transdermal microsystem, with the commercial CGMS unit and arterial blood draws. The BFIT was placed on carefully shaved skin as described above, and pressed onto the skin by a glass slide. The BFIT chip was visible through the slide and available for microscopic observation and filming during the ablation and assay phases of its operation. Since the BFIT chip is transparent any presence of interstitial fluid at the ablation site could be seen and recorded. For rats, 20 mJ pulses of 2.3 V were sufficient to ablate the stratum corneum and allow interstitial fluid to emerge, wetting the electrodes, but not damage in any way the underlying viable epidermis. These were the parameters that we designed for human use, and tested previously on living human graft skin. For pigs with their thicker epidermis, we found that 25 mJ of energy and 2.7 V were required. In the case of pigs we also washed and

patted dry the skin to remove any traces of soiling. The laser Doppler probe is an optical fiber in a plastic pedestal type mount that can be glued, or pushed onto the skin leaving the fiber pressed onto the skin perpendicular to the skin surface. The foot of the pedestal is about 6 cm in diameter, and it was placed as closely as possible to both the BFIT and CGMS sensors. It can be seen as the black device in Figure 8G and 8H below. Its role was to measure fluid velocities in the arteries and veins just under the skin's surface as a check that during hemorrhage circulation does not shut down to the tissues in which we are measuring the glucose concentrations present in interstitial fluid. Loss of circulation would mean that arterial concentrations no longer are in contact with these tissues and we would then expect no further equilibration between concentrations found in the arteries with those in interstitial fluid. For ease in BFIT micro-fabrication we chose to place two BFIT chips side by side, one with 25 glucose-sensitive cells and the other with 25 lactate-sensitive cells in the experiments when the two concentrations were logged simultaneously.

The CGMS sensor unit was placed according to the manufacturer's instructions. We disinfected the site, and used sterile gloves. Skin, including the fatty tissues beneath it, was pinched-up and the sensor's 2 cm-long stainless steel syringe together with the coaxial hollow plastic syringe containing the glucose-sensitive electrochemical electrodes was inserted at a glancing angle so as to be below the skin in the fatty tissues but not in the smooth muscle layers. Once in the desired location, the stainless steel syringe was removed, any blood or fluid swabbed away and the sensor was taped in place. The manufacturer recommends that the CGMS electrode be allowed to stabilize for one hour after implantation however we found that sensors can require much longer to stop drifting and providing fluctuating current values. After the first 60 minutes, a known blood glucose concentration was obtained by immediate (<5 min) analysis of freshly drawn arterial blood. This value was entered into the CGMS controller as a calibration point. The CGMS unit updates its measurements of currents every 10s, and records a time-averaged value in its memory along with a calculated glucose value every 300s, or 30 measurement cycles. One of the main interests in measuring glucose with the CGMS is that it is the only commercial system currently available, of which we are aware, that measures glucose using interstitial fluid. It has obtained FDA 510K approval for implanted use in humans for up to three days, and has been found to be "indicative" of blood glucose levels.

Finally, we employed the YSI 2700 analyzer beside the animal in surgery to assay with high (<5% error) precision the concentrations of glucose and lactate in arterial blood samples. This machine was preferred to point of care analytic tools such as the i-Stat hand-held analyzers or the Radiometer ABL 700 series blood gas machines for several reasons. Firstly, the latter analyzers are designed for use with whole human blood, and we are dealing with rats and pigs. The calibrations may be as much as 5% different. Secondly, the intended use and calibrations of the latter analyzers is for blood whose hemocrit is close to normal (30-50%). During resuscitation the subject animal's hemocrits can dip as low as 10%, far from calibrated ranges. We avoided these sources of error by measuring glucose and lactate concentrations in plasma as follows: Fifty μL samples of blood was taken from larger draws (1-5cc) immediately before any separation or clotting could occur, and were centrifuged to separate out the blood cells. Hemocrits were measured manually and immediately 12.5 μL blood plasma samples were introduced into the YSI analyzer. We strove in this way to keep any error in both blood glucose and blood lactate assays to less than 5%.

4.2 Non-Intrusiveness

Some of the tests we have performed on rats to prove the nonintrusiveness of the sampling technology are summarized in the images of Figure 6. In the sequence of four micrographs on the left we show pictures taken every 30 ms during a 30 ms 20 mJ pulse that ablates the stratum corneum. In the middle of each micrograph we see the serpentine structure of the heater (called TPS – thermal perforation system) in the 50 micron gap between gold conductor strips. The photograph is taken by a shallow depth of field optical microscope

through nearly 1 mm of living human graft skin. One can make out the outlines of the stratum corneum cells touching the plane of the BFIT chip surface, with a flattened slightly oval shape of about 50 microns in diameter. In the first picture of the sequence we see first the skin and heater before power is applied. Power is applied in the second picture, and some thermal expansion of the serpentine structure is visible as it heats, ultimately to 140° C. In the third picture we captured the first stratum corneum cell that ablates. Thirty milliseconds later, interstitial fluid is observed to wet the vicinity of the opening. In the middle photograph we zoom-out by a magnification factor 20X to see the full 5x5 array of individually addressed measurement cells. To establish the scales we show a 25-gauge syringe tip touching one of the sampling cells. Finally, in the pictures at the right of Figure 6 we show a stereo-zoom micrograph of the 50-micron diameter opening in the stratum corneum created by the BFIT visible once the chip is removed from the rat's skin surface. By way of comparison we show a picture of the rat's skin where a syringe has penetrated the skin. A cut of ½ mm is seen where the syringe cut into the skin, as well as a small amount of dried blood in the corner of the skin flap, and generalized swelling and bruising with a ½ mm diameter, at depth in tissues.

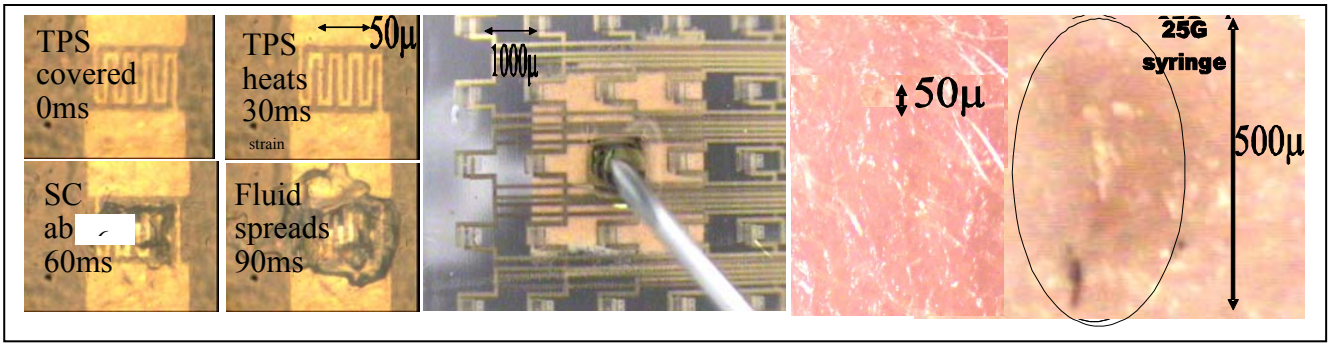

Figure 6. Non-intrusive sampling: **(left)** Sequence of 4 micrographs at time intervals of 30ms during application of a 20mJ pulse and ablation of the stratum corneum and contact with interstitial fluid, **(center)** zooming-out by 20x to see the matrix of 5x5 individually addressed measurement cells and a very fine 25gauge syringe, **(right)** micrograph of a S-D rat's skin comparing the puncture of the syringe to the healthy viable epidermis under BFIT's ablation.

4.3 Two Hemorrhagic Shock Experiments with Glucose Stress Testing on Rats (R16, R226)

We refer to the multivariable graphs and photo of Figure 7 below to give the details of these experiments. First looking at the photo of Figure 7D we see Rat 16 lying on its back with a BFIT pressed onto its shaved abdomen by a glass slide. Above it is the barrel of a microscope zoom lens and the tip of an optical fiber illuminator. The BFIT device is inserted into its ZIF micro-connector and a flexible 66-wire cable communicates to the microsystem controller, delivering current bursts for ablation and collecting electrochemical currents from the 25 separate glucose sensitive cells located on the device. To the right of the photo one sees the closed incisions in which are placed catheters to the femoral artery and vein. Carotid catheters are not visible, but one can see some of the electrical probes placed for measuring EKG and EEG. Some of the details of the hemorrhagic shock are given in the time chart of Figure 7A. The green line gives the mean arterial blood pressure (MBP [mmHg]) as a function of the time of day on which the experiment was conducted. The blue line provides a measurement of the shed blood volume (SBV) by measuring the weight of shed blood on a digital microbalance in grams as a function of time. The red line called marker identifies with its ticks the interesting physiological points of progress in the hemorrhage. From left to right, the first tick gives the moment when blood begins to be with drawn and the MBP begins its decline. The next three ticks correspond to the moments the SBV reach half maximum, maximum and half maximum again as blood

is first with drawn then pumped-back into the body. The pumping of blood is performed so as to keep the MBP at 40 during the controlled hemorrhage. About 40 minutes after resuscitation, at the final group of ticks, two ml of 300 mM glucose in isotonic saline is administered through the femoral arterial catheter. About 30 min later the rat dies. The blood glucose assays [mM] of the YSI analyzer are plotted together with the electrochemical currents registered from BFIT cells interrogated during the shock experiment. The YSI curve shows a slow increase from 3 to 4 mM before shedding blood, and the usual peak shape during the course of blood shedding and restoration, rising to 9 mM and declining to 7 mM, and then 3 mM again as glucose is delivered to the circulating system principally from the liver, metabolized and eliminated by the kidneys. At the point of glucose injection the concentration rises rapidly to 18 mM, falling to 8 mM at the animal's death. The first BFIT sensor G9 only operated for 15 min in interstitial fluid and followed the decline proportionately until a twitch from the rat moved the sensor and broke contact to the point of ablation. It took several minutes to open two new channels through the stratum corneum. G15 and G10 once again track proportionately (with the exception of the final reading from cell G10) the blood glucose concentration until the animal dies.

Figure 7C shows the CGMS currents in blue reported during the same time course. The sensor appears to drift to lower currents from the time it is implanted until the animal's death. Along the way there are some rises in current above the general decline. However, the peak in these rises does not correlate with either the time or magnitude of the arterial glucose concentrations. This sensor appears to fail to work correctly at all.

A second experiment was performed in a male rat R226. Prior to hemorrhage, two glucose injections were given, and after hemorrhage, like R16, another glucose injection was given. We will see that as we expect, before hemorrhage, the rat clears quickly in a few minutes the excess blood glucose and that this is simply slowed-down in the resuscitated rat. Figure 7E gives the measured MBP and SBV for the duration of the experiment. Looking at the MBP, we see that it rises, as does the base blood glucose during the first four hours of surgery, most likely due to a sympathetic response. The ticks on the marker line identify the instants that the three glucose injections are made as well as the moments of initial, half-maximum and maximum shed blood volume. In Figure 7F, the arterial blood concentrations and the BFIT electrochemical currents are presented. Focusing on the event of the first injection, the YSI measures a rise from 10 mM to 20 mM within a minute followed by a decrease to near 10 mM after 8 min, then a rise to 15 for an hour. The BFIT cell G1 began to track the rise, and then became an open circuit. We immediately switched to cell G5. Its current rose and declined simultaneously with the blood glucose level following the first injection, albeit at an attenuated level. That is the peak to valley change in current increases about 30% while the blood glucose level increases 100%. A second rise in glucose concentration is indicated by the BFIT G5 cell, but there are not sufficient blood analyses during that period to confirm that. Clearly by the sec, the G% cell no longer responds, its current remains flat up to and through the hemorrhagic shock. Following the shock, three cells were opened on a new chip, numbers G1, G2, and G3. No change was observed in any of the three cells at, or following the third injection up until death during a period when the blood glucose rises from 8 to 17 and falls back to 2 at death. With no response in three separate cells it appears that the interstitial fluid no longer communicates with the circulating blood. This is also seen in the lactate signal discussed below.

Figure 7G shows both the blood lactate assay concentrations and the current of lactate cell L13. These show very good correlation up until a moment following the second hemorrhage when the current becomes constant, exactly like the glucose concentrations in Figure 7F. The observed current changes by the same proportions as the blood lactate concentration. The final curve in Figure 7G shows the CGMS current together with the blood glucose concentration. The CGMS signal responds simultaneously with the first glucose injection and in direct proportionality, rising again, noisily after the blood glucose returns to normal. At this point the CGMS begins to drift downwards, misses the second and third injection blood glucose response. This is difficult to understand given that the sensor is intended to follow blood glucose for three days

following implantation. Yet it does correlate qualitatively with the observed BFIT signals. If the CGMS currents are accurate, then there are very significant changes in interstitial fluid concentrations compared to blood levels following major physiological changes like hemorrhagic shock.

4.4 Two Hemorrhagic Shock Experiments on Pigs (P21, P22)

The next two experiments involve single and double controlled hemorrhages in pigs with no glucose or drug injection. The results of the first experiment on pig 21 appear in Figure 8. Figures 8G and 8H show two views of the placement of the three sensors: BFIT, CGMS and Laser-Doppler. In Figure 8A shows the MBP and SBV traces. Looking at the sequence of ticks on the marker line from left to right, one sees the beginning, half maximum and maximum shed volume points of two successive controlled hemorrhages with minimum blood pressures maintained at 40mmHg. The laser-Doppler signal we logged scaled directly with the mean blood pressure signal. This indicates that blood continued to flow into the area in which our BFIT and CGMS sensors were placed throughout the experiment up until death. It also confirms that the surgical incision and placement of the catheter visible next to the BFIT in Figure 8H. In Figure 8B we show the measured currents in three BFIT cells actuated sequentially: G6, G21 and G25. Taken one after the other, they track well the YSI blood glucose assays. Blood would have to be drawn much more frequently to shed light on whether the BFIT current peaks in current follow blood glucose peaks. Referring back to the experiment with Rat 226, when blood was drawn every minute or two following a glucose injection, there was no lag between the two signals. This contrasts to the graph in Figure 8C of the CGMS current throughout the experiment where there is no correlation observed to the blood glucose curve.

The experiment with Pig 22 was longer that the previous one and the animal survived a second resuscitation. This is evident in Figure 8D where there are two shed blood volume peaks and a final blood draw until death. The tick marks on the marker line indicate sequentially the points of starting the bleed, half maximum volume, maximum volume, and finally when the shed blood volume is replaced by isotonic saline. After the first resuscitation the MBP slowly climbs back to 90 mmHg, its pre-hemorrhagic value. After the second resuscitation, the MBP reaches 70 mmHg. In the final and fatal hemorrhage, the MBP drops to zero. The blood glucose concentration during this time rises slowly from 4.5 to 6, with very slight increases during the shedding of blood. Three BFIT sensors operated during the experiment. None of the three track completely the blood glucose curve. This is in part because of the infrequency of blood draws. The G16 current curve shows a small increase in glucose during the first controlled hemorrhage, but does not decrease in the same way as the blood glucose. The cell G13 shows a flat response as does the blood glucose except for the abrupt step in current observed in the first few minutes. Finally, cell G6 begins by tracking a small decrease in glucose concentration following the second bleed. The shape of that curve is similar to that of G16 in which the decrease is very gradual. At the end of the fatal hemorrhage, the glucose current fell abruptly, similarly to the current drop of sensor G25 in the previous experiment in Figure 8E. The final graph of Figure 8G shows the measured CGMS currents throughout the experiment. That sensor seemed to drift continuously from 22 nA down to 17 nA while the blood glucose concentration increased continually. During the fatal hemorrhage, the CGMS signal dropped sharply by 65% as did the BFIT cell G6.

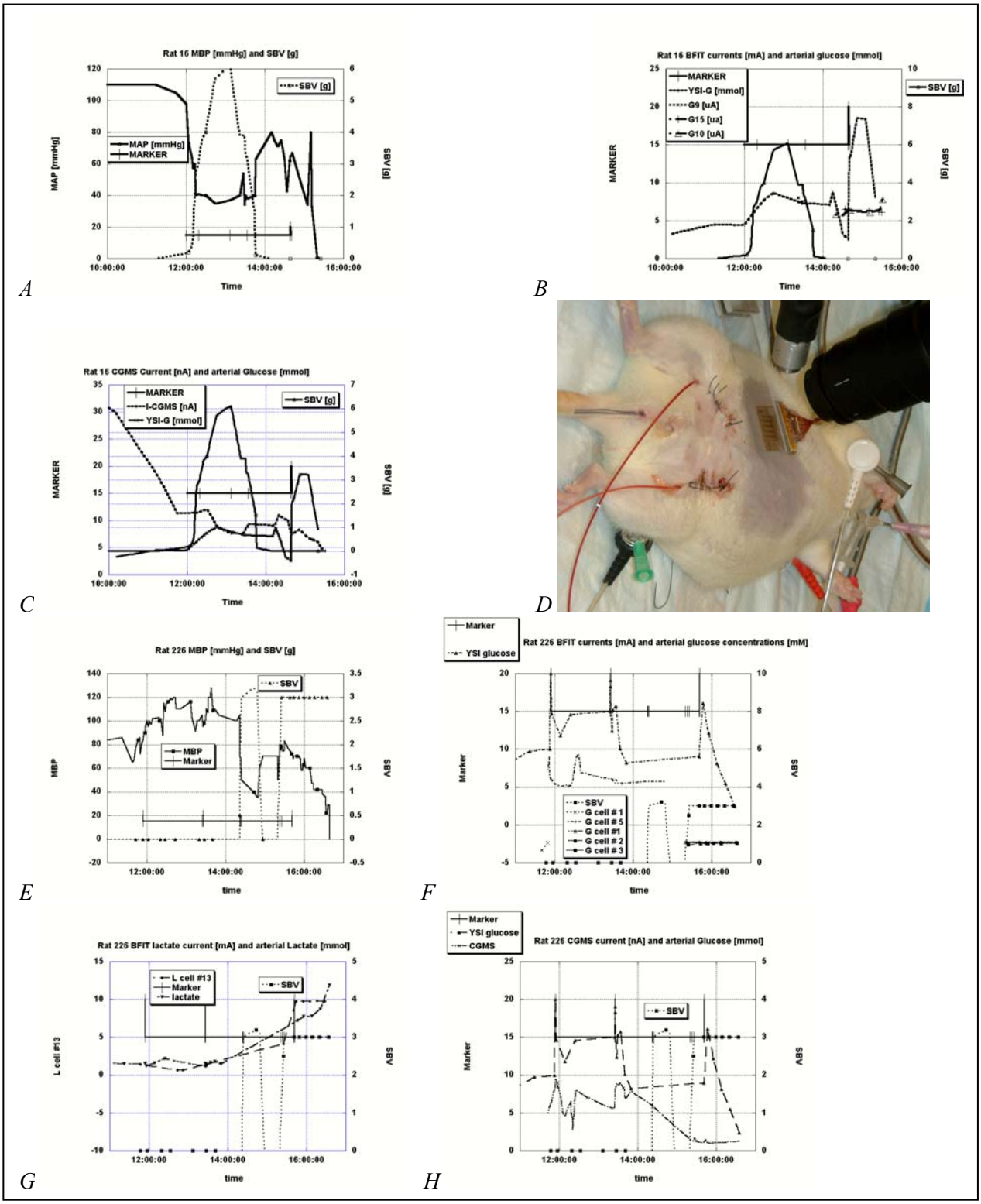

Figure 7: Two hemorrhagic shock experiments on rats.

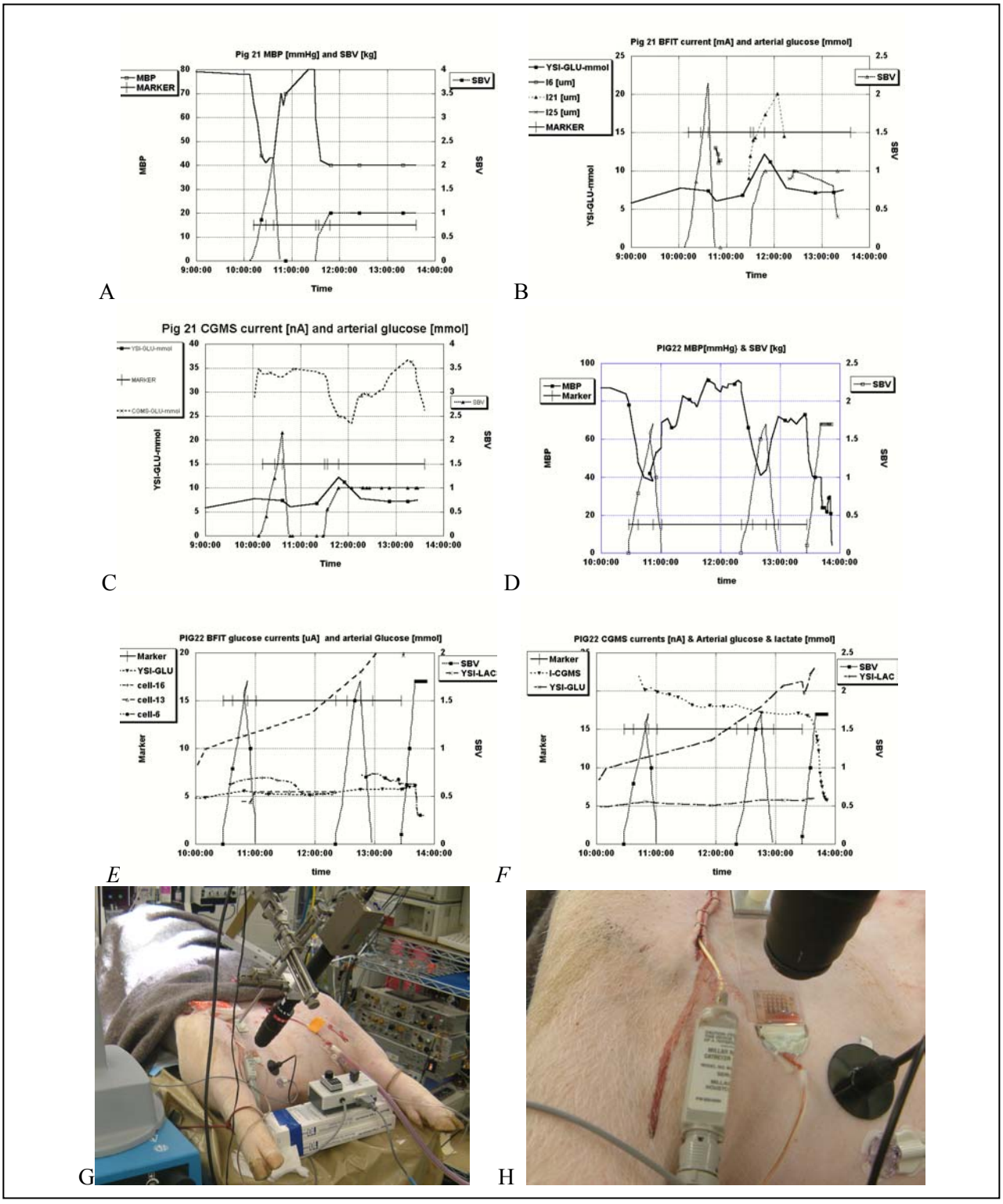

Figure 8. Two hemorrhagic shock experiments on pigs.

4.5 Two Hemorrhagic Shock Experiments with Adenosine A1 Receptor Inhibitor in Rats (R224, R225)

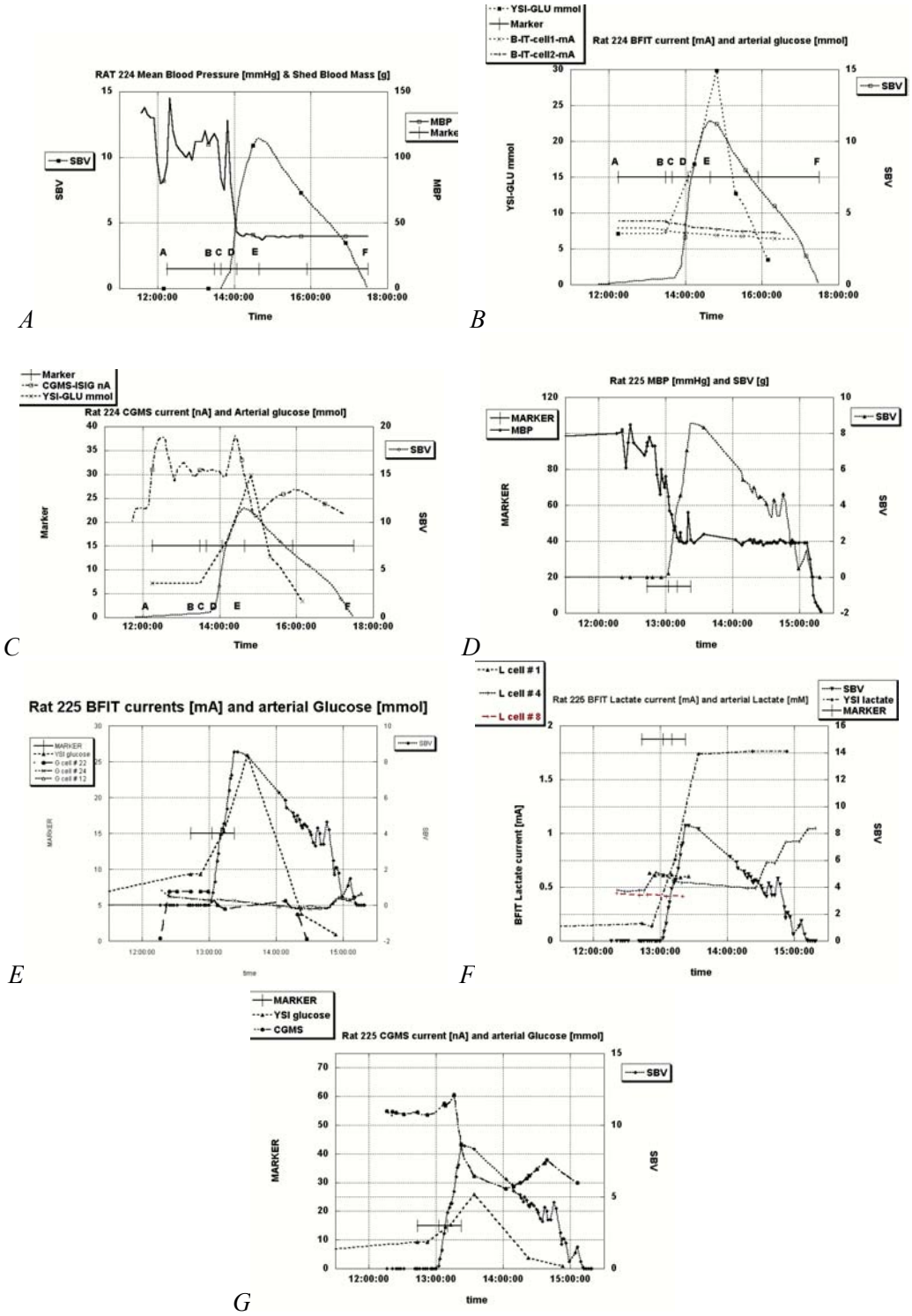

Figure 9. Two hemorrhagic shock experiments on rats.

This pair of hemorrhagic shock experiments is similar to the first pair, except for two changes: i) 10 min prior to the controlled hemorrhage, a 0.1 mg dose of theophylline is administered by arterial infusion, and ii) there is no resuscitation, the rat is maintained by controlled bleeding and infusion of heparinized blood at a MBP of 40 mmHg until death. One effect of this drug is to constrict blood vessels. One hypothesis is that vasoconstrictors can reduce the amount of resuscitation fluid required and improve survivability. We can not comment on this hypothesis and our observations are strictly limited to the ability of the BFIT and CGMS devices monitoring glucose in interstitial fluid to track blood. From this stand-point the drug treatment produces two new desirable effects: i) blood glucose and lactate concentrations increase dramatically – a factor of two higher than in previous experiments, and ii) the vasoconstriction effectively isolates the interstitial fluid from the blood for a period of about an hour until, near death, the constriction disappears and the blood and interstitial fluid concentrations can equilibrate. These represent new measuring challenges for a monitor both in terms of response-amplitude and frequency.

The first experiment on rat 224 is summarized in Figure 8A. Following the ticks on the marker line from left to right we see the following sequence of events: begin recording, drug injection, starting hemorrhage, half-maximum, and then maximum shed blood volume followed by half maximum and maximum resuscitation volumes. The latter event occurs just prior to death. Figure 8B gives the arterial blood glucose concentration and the BFIT glucose currents measured. Note that the cells G1 and G2 both track the blood glucose until the drug is administered. Then the blood concentration rises rapidly to 30 mM and drops-back to 4 mM. Both cells stopped recording just prior to death. But the glucose concentration in the interstitial fluid continues to decline very slightly: appearing to be cut-off from the concentrations in the blood. Figure 8C gives the corresponding CGMS currents measured. They appear to be quite noisy throughout the whole experiment. Time-averaging the currents leads to a response similar to the one recorded by the BFIT sensors in Figure 8B.

The final experiment on rat 225 repeats the same hemorrhage sequence as rat 224. In Figure 8D, we see that the MBP and SBV signals are smoother, indicating a more robust subject. Also the monitors were all kept recording for several minutes following death to explore novel effects in glucose concentration. Note the MBP is followed down to 0. Looking at Figure 8E we see that once again the blood glucose peaks sharply then drops to hypoglycemic levels. The BFIT sensors vary by about 10% one from another but reproduce the very slowly declining glucose current seen in Figure 8B above. Note that the cell G-22 suddenly decreases and tracks the blood glucose. This is confirmed by the tracking of lactate cell L4 as discussed below. The two other cells G12 and G24 have currents that begin to drift-up slightly.

Figure 8F gives the blood lactate concentration as well as the currents observed in three BFIT lactate cells. The blood lactate suddenly increases from a constant concentration following the drug injection then saturates at 14 mM. The BFIT cells L1, L4, and L8 track the blood lactate until drug injection when they begin to drift lower, likely being sealed-off from blood concentrations by the vasoconstriction. Shortly after drug injection, the rat began to move and cells L1 and L8 ceased to register current. Cell L4 continued to work and initially tracked the lactate rise, then relaxed downwards – again in an apparent isolation from the blood. However, at the precise moment when glucose cell G22 began to track the blood glucose, lactate cell L4 begins to track the blood lactate concentration.

The final curve, Figure 8G shows the electrochemical current response of the CGMS sensor. It appears to track neither the blood glucose, not any of the BFIT sensors.

5.0 CONCLUSIONS

We have demonstrated *in vitro* with human graft skin and *in vivo* with rats a prototype fieldable remote non-intrusive monitoring system for the assay of glucose and lactate in interstitial fluid. It has the flexibility to monitor almost any moderately hydrophilic/soluble bio-molecule of molecular weight less than 60k Daltons, as are commonly found in measurable concentrations in the interstitial fluid just under the skin's stratum corneum and in other body fluids such as saliva.

6.0 ACKOWLEDGEMENTS

The authors wish to thank Dr. Anand Gadre and Mr. Paul Goldey for their valuable assistance during the animal experiments, and to the DARPA/ARO project managers for their excellent support and encouragement throughout the years of this research and development: Drs. Robert J. Campbell, Abe Lee, Michael Krihak, and Anantha Krishnan.

7.0 REFERENCES

[1] DARPA/U.S. Army Research Office contract #, DAAD 19-00-1-0390 ; Drs. A. Lee, M. Krihak, A. Krishnan and R.J. Campbell, Project Managers

[2] USPTO application # 09/866,826, 05/30/00; Systems and Methods for Monitoring Health and Delivering Drugs Transdermally

[3] W.C. Shoemaker et al. (1996) Crit. Care Med. Vol24, pps12-s23

[4] F.J. Pearce et al. (1985) J. Surg. Research, Vol 39 , p390-8

[5] WPSM, USAMRMC/Military Operational Medicine Research Program/ Ft. Dietrich MD.

[6] Fabrication of an Epoxy based multi layer biofluidic dermal patch A. P Gadre, A. J. Nijdam, J. A. Garra, A. H. Monica, T. J. Long, C. Luo, M. C. Cheng, T. W. Schneider, R. C. White, M. Paranjape and J. F.Currie, Transducers 2003

[7] Multi polymer fabrication of a biofluidic transdermal sampling device, A.P. Gadre, Y. N. Srivastava, J. A. Garra, A. J. Nijdam, A. H. Monica, M. C. Cheng, C. Luo, T. W. Schneider, T. J. Long, R. C. White, M. Paranjape, J. F.Currie, MicroTAS 2003

[8] Fabrication of a fluid encapsulated dermal patch using multi-layered SU-8, A.P. Gadre, A. J. Nijdam, J. A. Garra, A. H. Monica, M. C. Cheng, C. Luo, Y. N. Srivastava, T.W. Schneider, T. J. Long, R. C. White, M. Paranjape, J.F.Currie, Accepted in Sensors and Actuators

[9] A Dry release technique for polymer Micro-TAS integration, M. C. Cheng, A. J. Nijdam, J. A. Garra, A. P. Gadre, T. W. Schneider, R.C. White, M. Paranjape, and J. F. Currie, MicroTAS 2003

[10] Polymethylmethacrylate as a fluid encapsulating membrane material in a micro fluidic device, Y. N. Srivastava, A. P. Gadre, J. A. Garra, A. J. Nijdam, A. H. Monica, M. C. Cheng, C. Luo, T. W. Schneider, T. J. Long, R. C. White, T. Hylton, M. Paranjape and J.F. Currie, Journal of Vacuum Science and technology 2004.

[11] M. Paranjape, J. Garra, S. Brida, T. Schneider, R. White, J. Currie, "A PDMS Dermal Patch for Non-Intrusive Transdermal Glucose Sensing", Sensors and Actuators – A104, pp. 195-204, 2003

[12] T. Schneider, R.C. White, M. Cheng, J. Garra, M. Paranjape, J. Currie, "MEMS Bubble Actuated Valve for Interstitial Glucose Sensing", Proceedings of the Electrochemical Society – Symposium on Microfabricated Systems and MEMS IV, pp. 153-160, 2002.

[13] J. Garra, T. Long, J. Currie, T. Schneider, R. White, M. Paranjape, "Dry Etching of Polydimethylsiloxane for Microfluidic Systems", Journal of Vacuum Science and Technology, **A20**, pp. 975-982, 2002

[14] C. Luo, J. Garra, T. Schneider, R. White, J. Currie, and M. Paranjape, "Determining Local Residual Strains of Polydimethylsiloxane Using Ink Dots, and Stiffening Polydimethylsiloxane Using SU-8 Particles", Journal of Micromechanics and Microengineering, **12,** pp. 677-681, 2002

[15] C. Luo, T. Schneider, R. White, M. Paranjape, and J. Currie, "A FEA Deflection-Testing Method to Determine Poisson's Ratio for MEMS Applications", Journal of Micromechanics and Microengineering, 13, pp. 129-133, 2002

[16] POC: Dr. James L. Holeman, Sr.President: jholeman@HolemanScientific.com

[17] HFM-109/RSY papers by Bodo #P03, Baranyi #12, Oliver #P22, Lee #25, and Van Albert #27.